



## OPEN ACCESS

EDITED BY  
Zizheng Guo,  
Hebei University of Technology, China

REVIEWED BY  
Jun He,  
Hebei University of Technology, China  
Bing Bai,  
Beijing Jiaotong University, China

\*CORRESPONDENCE  
Chengyuan Dai,  
✉ 2016015@glut.edu.cn

SPECIALTY SECTION  
This article was submitted to  
Environmental Informatics and  
Remote Sensing,  
a section of the journal  
Frontiers in Earth Science

RECEIVED 30 November 2022  
ACCEPTED 19 January 2023  
PUBLISHED 03 February 2023

CITATION  
Zhang X, Dai C, Li W and Chen Y (2023),  
Prediction of compressive strength of  
recycled aggregate concrete using  
machine learning and Bayesian  
optimization methods.  
*Front. Earth Sci.* 11:1112105.  
doi: 10.3389/feart.2023.1112105

COPYRIGHT  
© 2023 Zhang, Dai, Li and Chen. This is an  
open-access article distributed under the  
terms of the [Creative Commons  
Attribution License \(CC BY\)](https://creativecommons.org/licenses/by/4.0/). The use,  
distribution or reproduction in other  
forums is permitted, provided the original  
author(s) and the copyright owner(s) are  
credited and that the original publication in  
this journal is cited, in accordance with  
accepted academic practice. No use,  
distribution or reproduction is permitted  
which does not comply with these terms.

# Prediction of compressive strength of recycled aggregate concrete using machine learning and Bayesian optimization methods

Xinyi Zhang<sup>2</sup>, Chengyuan Dai<sup>1\*</sup>, Weiyu Li<sup>2</sup> and Yang Chen<sup>2</sup>

<sup>1</sup>Key Laboratory of Building New Energy and Building Energy Saving, Guilin University of Technology, Guilin, China, <sup>2</sup>School of Civil and Architectural Engineering, Guilin University of Technology, Guilin, China

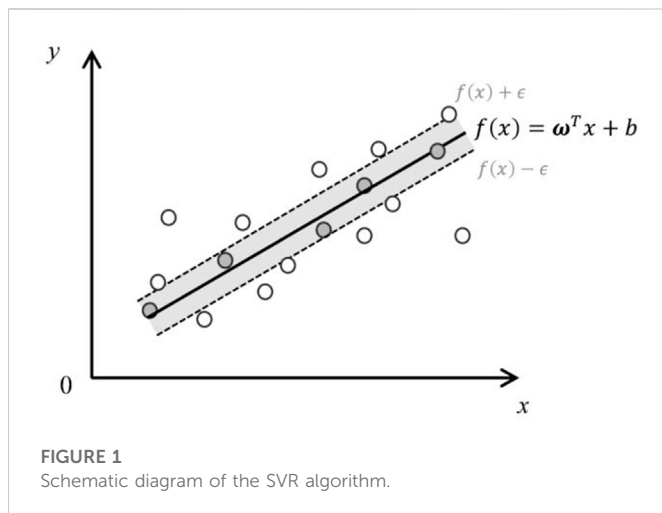
With the sustainable development of the construction industry, recycled aggregate (RA) has been widely used in concrete preparation to reduce the environmental impact of construction waste. Compressive strength is an essential measure of the performance of recycled aggregate concrete (RAC). In order to understand the correspondence between relevant factors and the compressive strength of recycled concrete and accurately predict the compressive strength of RAC, this paper establishes a model for predicting the compressive strength of RAC using machine learning and hyperparameter optimization techniques. RAC experimental data from published literature as the dataset, extreme gradient boosting (XGBoost), random forest (RF), K-nearest neighbour (KNN), support vector machine regression Support Vector Regression (SVR), and gradient boosted decision tree (GBDT) RAC compressive strength prediction models were developed. The models were validated and compared using correlation coefficients ( $R^2$ ), Root Mean Square Error (RMSE), mean absolute error (MAE), and the gap between the experimental results of the predicted outcomes. In particular, The effects of different hyperparameter optimization techniques (Grid search, Random search, Bayesian optimization-Tree-structured Parzen Estimator, Bayesian optimization- Gaussian Process Regression) on model prediction efficiency and prediction accuracy were investigated. The results show that the optimal combination of hyperparameters can be searched in the shortest time using the Bayesian optimization algorithm based on TPE (Tree-structured Parzen Estimator); the BO-TPE-GBDT RAC compressive strength prediction model has higher prediction accuracy and generalisation ability. This high-performance compressive strength prediction model provides a basis for RAC's research and practice and a new way to predict the performance of RAC.

## KEYWORDS

machine learning, recycled coarse aggregate concrete, compressive strength prediction, Bayesian optimization, ensemble learning

## 1 Introduction

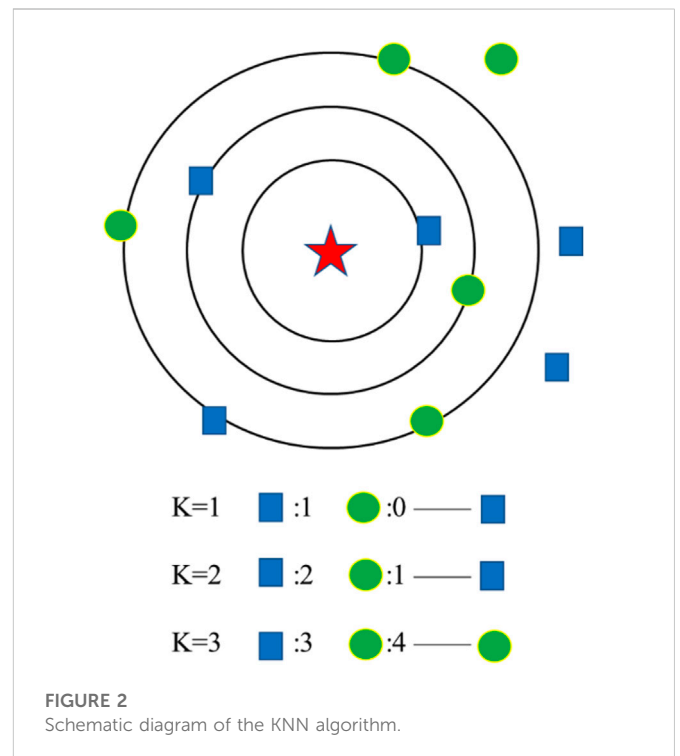
With the awakening of sustainable development awareness in the construction industry, green and low-carbon development has become an industry consensus (Spence and Mulligan, 1995; Sev, 2009; Giesekam et al., 2016; Zhang et al., 2017; Xia et al., 2018; Zhang et al., 2018). In recent decades, China's economy and urbanisation have grown rapidly. In urbanisation, many natural resources are used for new buildings, leading to the depletion of natural resources. On the other hand, construction waste from demolishing old buildings is difficult to dispose of and causes environmental pollution. Therefore, exploring the recycling value of construction waste has become a crucial step in the sustainable development of the construction industry. Recycled



aggregate concrete (RAC) is undoubtedly the best example of construction waste recycling. RAC processes waste concrete into recycled concrete aggregates, replacing NA such as sand and gravel in regular concrete. It conserves natural resources and effectively disposes of construction waste, reducing environmental pollution and land resources occupied by construction waste.

Many authors have evaluated the compressive strength of RAC, which is a valid property that has an important impact on the durability of RAC (Bai et al., 2020). The compressive strength of RAC is affected by numerous factors, such as the replacement rate of RA (Rakshvir and Barai, 2006; Gull, 2011), and the water-to-cement ratio (Meng et al., 2021; Ying et al., 2022), coarse aggregate type, coarse aggregate crushing rate, adherent mortar content, and moisture status (Shi et al., 2012; Silva et al., 2015). It is not appropriate to study influence factors independently, as the compressive strength of the RAC is a function of many interacting influence factors. However, the compressive strength of RAC is obtained by conditioning specimens for a specified period and performing tests, which are lengthy and costly in terms of the experimental period and material. There is a complex non-linear relationship between the compressive strength of RAC and the influencing factors, and new methods are needed to accurately reflect and accurately clarify the correlation between these influencing factors.

The rapid development of computer technology provides many facilities for solving engineering problems (Guo et al., 2020b; Wang et al., 2022a; Wang et al., 2022b). At the same time, machine learning (ML) technology has made great progress. With its efficient data processing capability and accurate data prediction ability, ML technology has rapidly become popular in traditional engineering. ML has been applied to predict various properties of concrete. Artificial neural network (ANN) often used to predict RAC compressive strength (Duan et al., 2013). Developed ANN models on the Matlab platform for predicting the compressive strength of concrete with different types and sources of RA. Show how the ANN model outperformed the Model Tree (MT) and Non-linear Regression (NLR) present in predicting concrete strength (Khademi et al., 2016). Used three different algorithms to predict the compressive strength of RAC, and the results showed that the ANN and adaptive neuro-fuzzy inference system (ANFIS) models could accurately predict the compressive strength of RAC. Mixes. Catherina et al. developed a



prediction model for the compressive strength of recycled aggregate concrete based on the ANN and Cuckoo Search Method (CSM) algorithms (Catherina and Chella, 2021). Although ANN shows good non-linear mapping ability, it also has some areas for improvement, including slow convergence, excessive learning and local optimization, which will affect the accuracy and efficiency of prediction.

ML methods rely on hyperparameter configuration. The choice of hyperparameters directly determines the model's performance and computation time. In hyperparameter optimization, the primary methods are the empirical method, grid search, random grid search, swarm intelligence optimization algorithm and Bayesian optimization algorithms. The advanced optimization framework Bayesian optimization algorithm was used to optimize the hyperparameters of the shear load capacity prediction model for SVR fiber-reinforced plastics (FRP) reinforced concrete members (Alam et al., 2021). The BOA-SVR model determined the optimal parameters in less time than other methods (Nunez et al., 2020). (Alhakeem et al., 2022) used a grid search method to optimize the GBRT hyperparameters to obtain a highly accurate predictive model for the compressive strength of the RAC (Guo et al., 2020a). Optimized BP models using Particle Swarm Optimization (PSO) and Grey Wolf Optimizer (GWO) to predict the non-linear relationship between random displacement and trigger factors in landslide displacement, providing a solid basis for early warning. The prediction models will have different prediction accuracies under other hyperparameter configuration methods. When the model is complex and the hyperparameters are increased, it requires a lot of computational resources and time. Exploring Various hyperparameter configuration methods has an important impact on the accuracy and modelling efficiency of the RAC compressive strength prediction model.

This paper developed XGBoost, RF, KNN, SVR and GBDT algorithm models to predict the compressive strength of RAC using hyperparameter

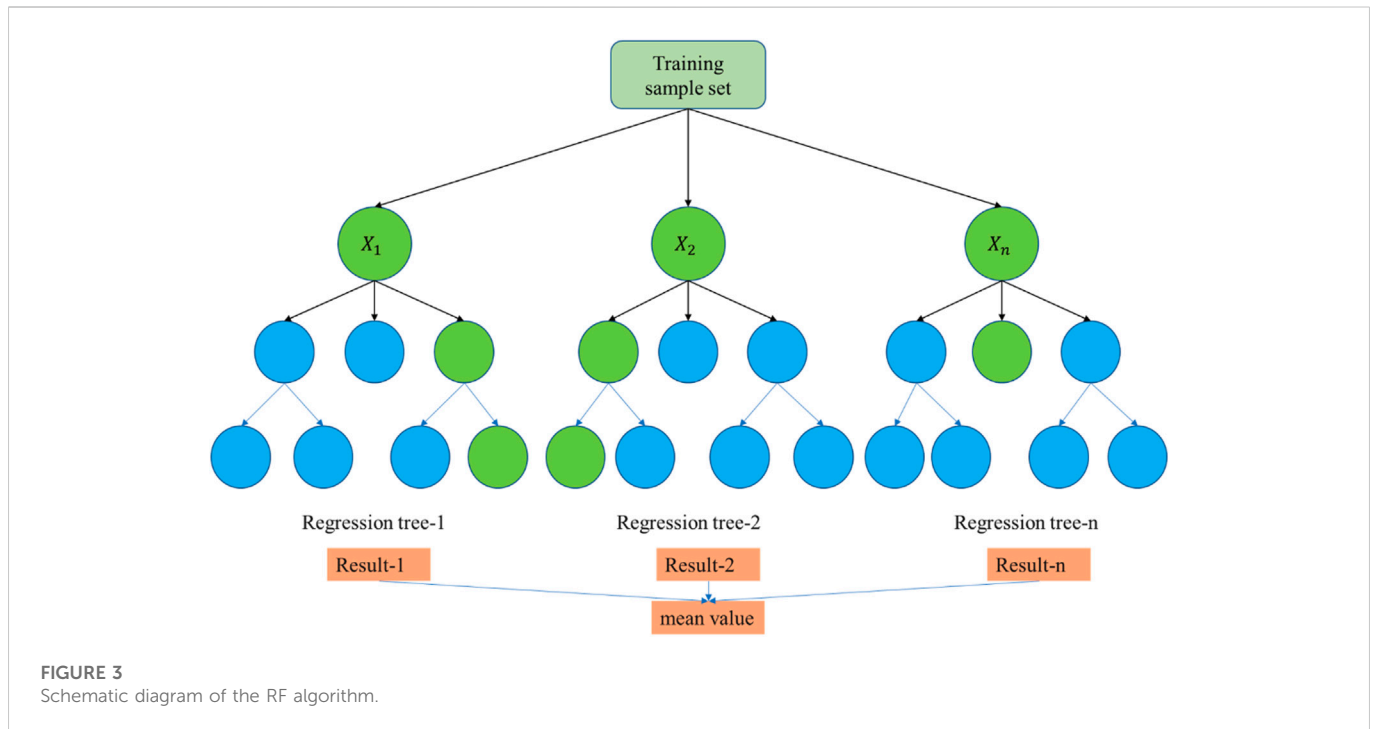


FIGURE 3 Schematic diagram of the RF algorithm.

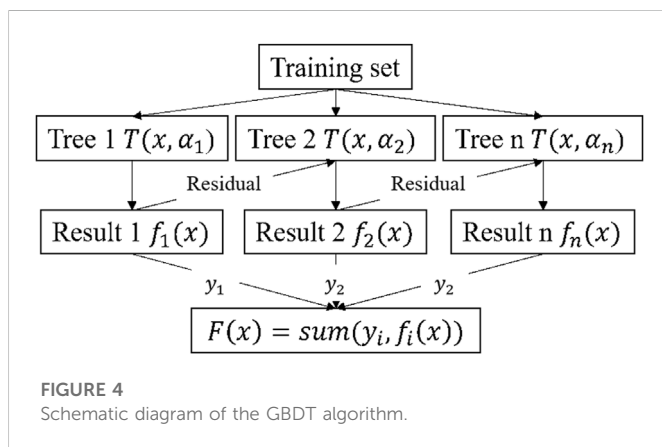


FIGURE 4 Schematic diagram of the GBDT algorithm.

optimization with Grid search, Random search, Bayesian optimization-Tree-structured Parzen Estimator, Bayesian optimization-Gaussian Process Regression methods. Twelve key factors, including effective water-cement ratio ( $w_{eff}/c$ ), aggregate-cement ratio ( $a/c$ ), RCA replacement ratio ( $\rho$ ), Parent concrete strength (PCS), nominal maximum RA size ( $\delta R$ ), nominal maximum NA size ( $\delta N$ ), bulk density of RCA (mR), bulk density of NA (mN), water absorption of RCA (rR), water absorption of NA (rN), Los Angeles abrasion index of RCA (lR), Los Angeles abrasion index of NA (lN) were used to predict the compressive strength of RAC. The prediction accuracy of the proposed models was evaluated in terms of evaluation indicators such as the coefficient of determination ( $R^2$ ), mean absolute error (MAE), Root Mean Square Error (RMSE), and the RAC compressive strength prediction model with the highest accuracy was selected. At the same time, the time spent by different hyperparameter optimization methods and the degree of model optimization is calculated, and the hyperparameter optimization method with high efficiency and good

results is selected. Although this paper only discusses the use of machine learning and hyperparametric optimization methods for the compressive strength of RAC, the model proposed in this paper can be easily extended to predict other mechanical capacities of RAC. Therefore, the machine learning approach proposed in this paper can be widely applied to the construction industry.

## 2 Machine learning methods

### 2.1 Support vector regression (SVR)

Support Vector Regression (SVR) (Smola and Schölkopf, 2004) is a supervised learning algorithm for predicting discrete values. The schematic diagram of the SVR algorithm is shown in Figure 1. The basic idea of SVR is to find a regression plane such that the total distance of all sample points to the plane is minimized. Achieving this goal requires mapping linearly indistinguishable low-dimensional data to a higher-dimensional space with the help of kernel functions to make them linearly distinguishable. SVR has the robustness to outliers, excellent generalization ability, strong learning ability for high-dimensional data, and high prediction accuracy (Vapnik et al., 1996; Schölkopf et al., 2000; Basak et al., 2007; Awad and Khanna, 2015) The SVR problem can be formalized as the following equation:

$$\min \frac{1}{2} \|\omega\|^2 + C \sum_{i=1}^m L(y_i, f(x_i)) \tag{1}$$

$$\begin{cases} \frac{1}{2} \|\omega\|^2 + C \sum_{i=1}^m (\lambda_i^+ + \lambda_i^-) \\ \text{s.t.} \begin{cases} y_i - f(x_i) \leq \epsilon + \lambda_i^+ \\ f(x_i) - y_i \leq \epsilon + \lambda_i^- \end{cases} \end{cases} \tag{2}$$

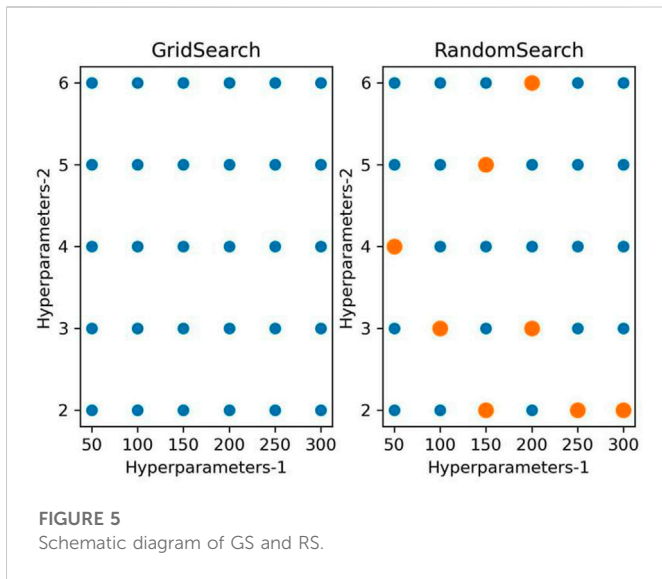


FIGURE 5 Schematic diagram of GS and RS.

Where,  $\omega$  is a vector, which determines the slope of the fitted line;  $C$  is regularization coefficient;  $L(y_i, f(x_i))$  is insensitive loss function;  $\lambda_i^+, \lambda_i^- (i = 1, 2 \dots n)$  relaxation variable;  $\epsilon$  is coefficient related to the interval band;  $f(x_i)$  is a fitted value;  $y_i$  is a sample true value.

### 2.2 K-nearest neighbor (KNN)

K-Nearest Neighbor (KNN) (Peterson, 2009) is an instance-based learning model. The schematic diagram of the KNN algorithm is shown in Figure 2. The core idea of the KNN algorithm is that a sample is classified into a category if most of its K nearest neighbors in the

feature space belong to that category. When using KNN to calculate the predicted value of a data point, the model selects the K nearest data points from the training data set and uses their mean values as the predicted value of the new data point. The KNN algorithm, which does not require estimation of parameters, does not require training and is simple and easy to implement (Ray, 2019; Sen et al., 2020).

### 2.3 Random forest (RF)

Random forests (Breiman, 2001) are ensemble learning algorithms that contain multiple decision trees. The schematic diagram of the RF algorithm is shown in Figure 3. The decision trees are grown randomly, and a randomly selected fraction of the samples brought back for release from the training data is used to construct the decision trees. Similarly, a portion of the features is randomly selected for training. Each tree has different samples and features, and the result differs. When dealing with classification problems, the random forest prediction category is the plurality of the class to which the random forest prediction sample units belong. When dealing with regression problems, the output value is the average of all tree predictions. The random forest algorithm takes less time, is less prone to overfitting, can handle high-dimensional data with more features, and is the algorithm with higher accuracy (Liu et al., 2012; Yuan et al., 2022).

### 2.4 Gradient boosting decision tree algorithm (GBDT)

Gradient Boosting Decision Tree (Friedman, 2001), which is a representative algorithm in boosting and the most used ML algorithm in the industry. The schematic diagram of the GBDT algorithm is shown in Figure 4. GBDT can flexibly handle various types of data,

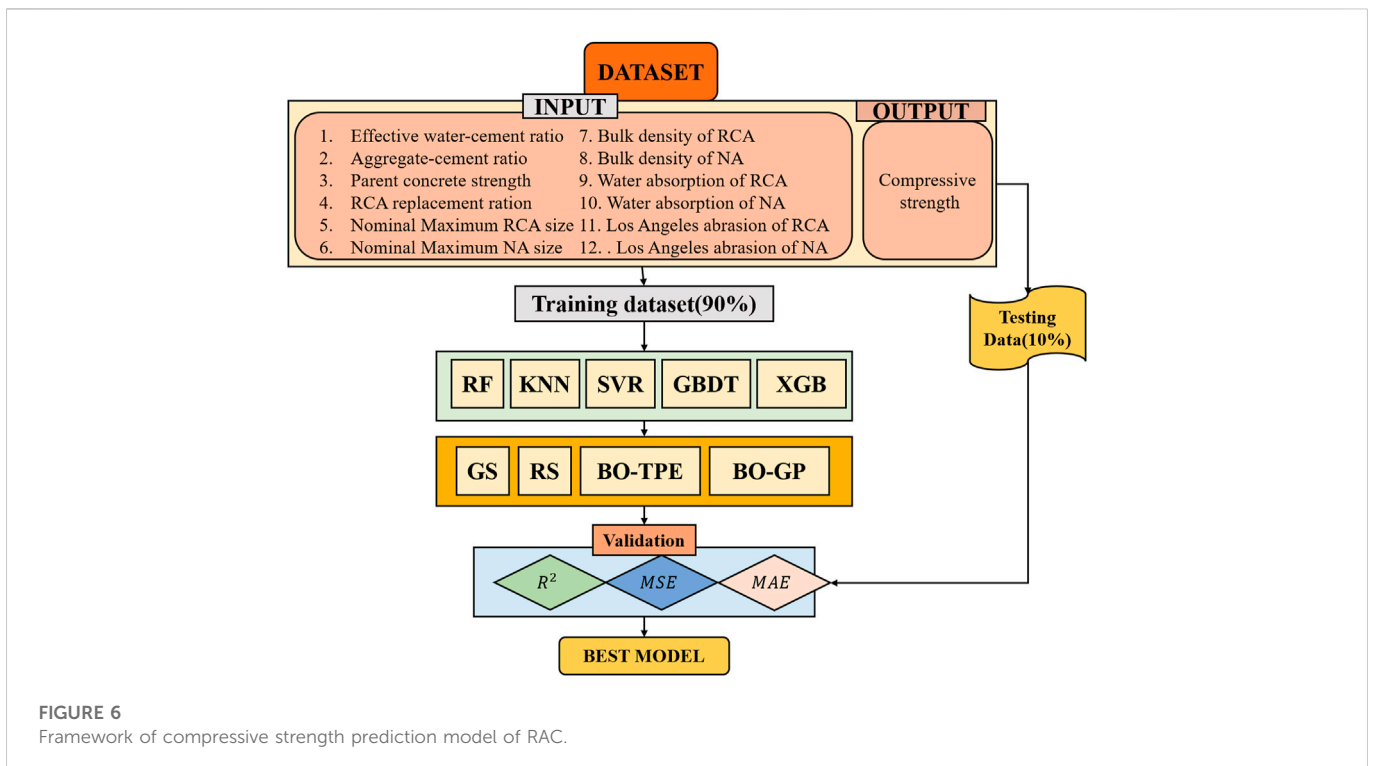


FIGURE 6 Framework of compressive strength prediction model of RAC.

TABLE 1 Description of data used in this study.

	Unit	Quantity	Mean	Median	Minimum	Maximum
$W_{eff}/C$	-	521	0.49	0.490	0.190	0.870
$a/c$	-	521	3.09	3	1.65	6.50
$\rho$	%	521	51.07	50	1.50	100
PSC	MPa	521	6.13	0	0	100
$\delta_R$	mm	521	21.35	20	0	32
$\delta_N$	mm	521	21.76	20	10	38
$m_R$	kg·m <sup>3</sup>	521	1,657.29	2,320	10	2,880
$m_N$	kg·m <sup>3</sup>	521	1,535.76	2,540	0	2,970
$r_R$	%	521	3.534	4.100	0	11.90
$r_N$	%	521	0.60	0.30	0	2.50
$l_R$	-	521	6.72	0	0	42
$l_N$	-	521	4.76	0	0	32
Compressive strength	MPa	521	43.19	41.5	15.464	108.50

including continuous and discrete values, and has the advantages of high efficiency, nominal missing values, easy model construction, high training accuracy, and good generalization ability. GBDT consists of two parts: Decision Tree (Quinlan, 1986), and Gradient Boosting (Freund et al., 1999).

The value of the negative gradient of the loss function in the current model is used as an approximation of the residuals of the boosted tree algorithm in the regression problem. That is, the iterative decision tree uses the residuals formed after the result of the previous tree construction as input data to construct the next subtree when constructing trees; the final prediction results are obtained by accumulating the subtree prediction results in the order of construction (Liang et al., 2020).

### 2.5 Extreme gradient boosting algorithm (XGBoost)

Extreme Boosting Tree (XGBoost) (Chen and Guestrin, 2016) is an ensemble algorithm based on Decision Trees, an upgrade of the Gradient Boosting Decision Tree algorithm. By constructing weak learners, continuously iterating to reduce the residuals of the last iteration, and accumulating the results of multiple weak learners as the final prediction output, XGBoost achieves a balance between the accuracy and complexity of the Tree model through loss functions and regularization items. At the same time, it greatly reduces the complexity of the model and improves the efficiency of the model operation (Li and Chen, 2020; Liang et al., 2020).

XGBoost is a ML algorithm based on the additive model framework, which uses a forward distribution algorithm and Regression Trees as the base learners. An optimal solution is sought for each Regression Tree to gradually approximate the optimal loss function. Expressed as Eq. 3 (Friedman, 2001).

$$\hat{y}_i^{(k)} = \sum_{j=1}^{k-1} f_j(x_i) + f_j^{(k)}(x_i) \tag{3}$$

Where,  $\hat{y}_i^{(k)}$  represents the predicted value of the  $i$  th sample;  $f_j(x_i)$  is the regression  $j$  th tree, and is  $x_i$  the number of base learners;  $\sum_{j=1}^{k-1} f_j(x_i)$  is the cumulative result of the previous  $k - 1$  regression trees; and  $f_j^{(k)}(x_i)$  is the current  $k$  th regression tree to be optimized.

In the XGBoost algorithm, the objective function is specific to each tree. For an arbitrary tree, the objective function has two components; one is an arbitrarily differentiable loss function that controls the empirical risk of the model. The remaining component contains the model complexity. Expressed as Eqs. 4, 5 (Chen and Guestrin, 2016).

$$Obj^{(t)} = \sum_{i=1}^N l(y_i, \hat{y}_i^{(t)}) + \sum_{j=1}^t \Omega(f_j) \tag{4}$$

$$\approx \sum_{i=1}^N l(y_i, \hat{y}_i^{t-1} + f_t(x_i)) + \Omega(f_j) \tag{5}$$

Where,  $\hat{y}_i^{(t)}$  is the predicted value of the  $i$  th sample;  $y_i$  is the true value;  $N$  is the number of samples;  $l(y_i, \hat{y}_i^{(t)})$  is the loss function;  $\sum_{j=1}^t \Omega(f_j)$  is the regularization item.

Splitting the objective function with the sample as the objective into one with the leaf nodes as the objective and substituting the second-order Taylor expansion formula into the objective function yields (Chen and Guestrin, 2016):

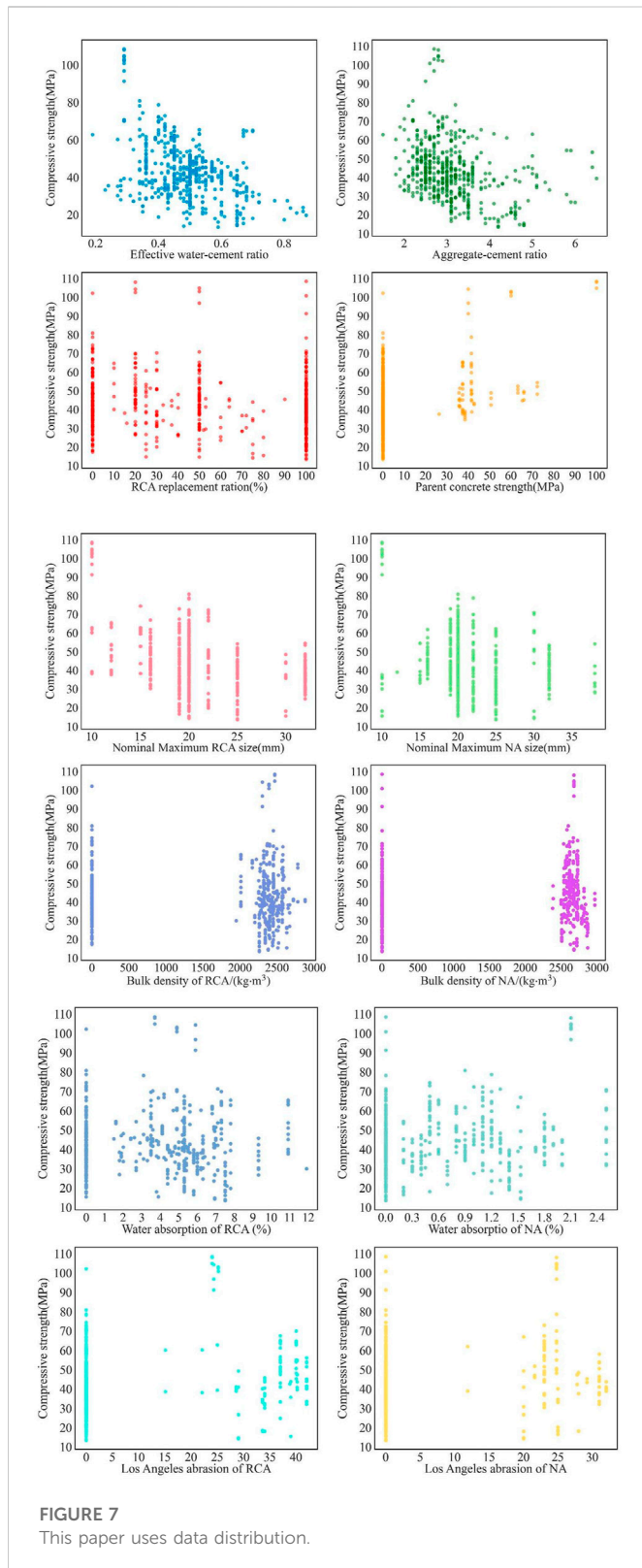
$$Obj^{(t)} = \sum_{j=1}^T \left[ \left( \sum_{i \in I_j} g_i \right) w_j + \frac{1}{2} \left( \sum_{i \in I_j} h_i + \lambda \right) w_j^2 \right] + \gamma T \tag{6}$$

$$\approx \sum_{j=1}^T \left( w_j + G_j \right) + \frac{1}{2} \left( \lambda + H_j \right) + \gamma T \tag{7}$$

Where,  $g_i = \partial_{\hat{y}_i^{(t-1)}} l(y_i, \hat{y}_i^{t-1})$ ,  $h_i = \partial_{\hat{y}_i^{(t-1)}}^2 l(y_i, \hat{y}_i^{t-1})$ ,  $G_j = \sum_{i \in I_j} g_i$ ,  $H_j = \sum_{i \in I_j} h_i$

Minimize the objective function to obtain the predicted values of leaf nodes; minimize the objective function  $Obj^{(t)*}$ , Expressed as Eqs. 8, 9 (Chen and Guestrin, 2016).

$$w_j^* = -\frac{G_j}{H_j + \lambda} \tag{8}$$



$$Obj^{(t)*} = \min Obj^{(t)} = \gamma T - \frac{1}{2} \sum_{j=1}^T \frac{G_j^2}{H_j + \lambda} \quad (9)$$

The key problem of the decision tree growth process is how to split the nodes. The XGBoost algorithm adopts a greedy strategy. For each leaf node division, the structural fraction gain is calculated, and the

point with the largest gain is selected for branching. Expressed as Eq 10 (Chen and Guestrin, 2016).

$$gain = \frac{1}{2} \left[ \frac{G_L^2}{H_L + \lambda} + \frac{G_R^2}{H_R + \lambda} + \frac{(G_L + G_R)^2}{H_L + H_R + \lambda} \right] - \gamma \quad (10)$$

Where  $\frac{G_L^2}{H_L + \lambda}$  is the structure fraction of the left node,  $\frac{G_R^2}{H_R + \lambda}$  is the structure fraction of the right node, and  $\frac{(G_L + G_R)^2}{H_L + H_R + \lambda}$  the structure fraction of the parent node.

## 2.6 Hyperparameter configuration method

Grid search (GS) and random search (RS) (Feurer and Hutter, 2019) are the most common hyperparameter configuration methods. The schematic diagram of GS and RS is shown in Figure 5. GS brings all parameter combinations in the parameter space into the model for training and finally selects the best-performing hyperparameter combination (Bergstra et al., 2011). The larger the parameter space, the greater the arithmetic power and time required for GS. The computational effort needed for grid search increases exponentially when the parameter dimension rises. RS does not use the whole hyperparameter space and constructs a parameter subspace using partial parameter combinations to search within the subspace, which improves the computational speed yet ensures the accuracy of the search. For high-dimensional data, random search is more effective than grid search.

Unlike the enumeration idea of GS and RS, Bayesian Optimization (BO) is based on the *a priori* idea. The core idea of BO is to use the prior probability of the objective function and known observation points to update the posterior probability distribution and then find the next minimal value point with a more posterior probability distribution and get the optimal hyperparameter after numerous iterations. The later hyperparameters are taken based on the results of the previous hyperparameters so that the best combination of hyperparameters can be configured in less time. BO is an application of machine learning automation that aims to configure hyperparameters automatically to achieve the best performance and reduce the human effort required to apply machine learning (Bergstra and Bengio, 2012; Eggenberger et al., 2015). BO can be expressed as the following equation:

$$x^* = \operatorname{argmax}_{x \in \chi} f(x) \quad (11)$$

where  $x^*$  is the optimal hyper-parameter combination,  $\chi$  is the parameter space, and  $f(x)$  is the objective function.

The key steps in BO are the probabilistic surrogate model and the acquisition function. The probabilistic proxy model builds a probability distribution model based on the existing history data; the acquisition function is used to select the basis for the next parameter combination and continuously adds different parameter combinations to the probabilistic surrogate model until the maximum number of iterations is reached.

The main difference between different Bayesian optimization methods lies in the probabilistic agent models and collection functions, main including Gaussian process (GP), and tree-structured Parzen estimators (TPE) models (Ozaki et al., 2020).

GP brings much convenience to modeling tasks in machine learning and statistics, and it can be used to specify functional distributions without the need for a specific functional form

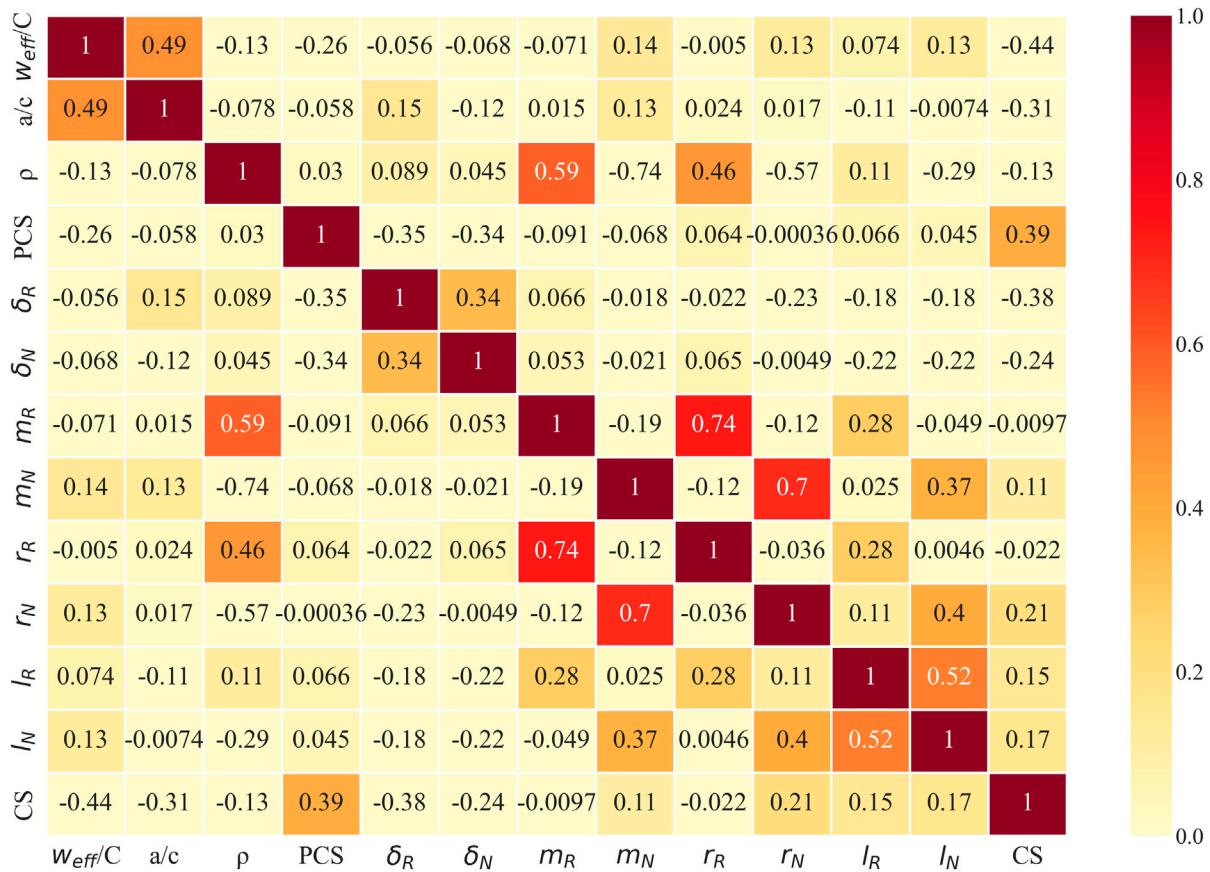


FIGURE 8 Input parameter data distribution Multi-correlation matrix of the input parameters and output.

(Rasmussen and Nickisch, 2010). Assume that the hyperparameters to be optimized are  $X = \{X_1, X_2, \dots, X_t\}$  and the dataset obtained after BO-GP iteration is  $D_t = \{(x_1, f(x_1)), (x_2, f(x_2)), \dots, (x_t, f(x_t))\}$ . The Gaussian process assumes that the observation points obey a Gaussian distribution, and the expression is as follows:

$$f(x_{1:t}) \sim GP(\mu(x_{1:t}), \sum(x_{1:t}, x_{1:t})) \tag{12}$$

$$\sum(x_{1:t}, x_{1:t}) = \begin{bmatrix} k(x_1, x_1) & \dots & k(x_1, x_t) \\ \vdots & \ddots & \vdots \\ k(x_t, x_1) & \dots & k(x_t, x_t) \end{bmatrix} \tag{13}$$

From Bayes theorem:

$$P(f(x_{t+1})|f(x_{1:t})) \propto P(f(x_{1:t})|f(x_{t+1}))P(f(x_{t+1})) \tag{14}$$

The optimal hyperparameters are finally obtained by continuously updating the iteration to make  $X_{min} = X_{t+1}$ .

TPE utilizes tree-structured adaptive Parzen estimators that handle discrete, categorical, and conditional variables with lower computational complexity than GP (Rasmussen, 2003). It shows better performance in complex parameter search space problems (Bergstra et al., 2013). The procedure is as follows.

$$P(x|y) = \begin{cases} l(x) & \text{if } y^* > y \\ g(x) & \text{if } y \geq y^* \end{cases} \tag{15}$$

Where  $x$  is the observation,  $y^* = \min\{x_1, f(x_1), \dots, (x_t, f(x_t))\}$  is the optimal value in the observation threshold;  $l(x)$  is the density estimate of the loss function of observation  $x$  less than  $y^*$ ; and  $g(x)$  indicates the density composition of the loss function of observation  $x_i$  greater than or equal to  $y^*$ .

The collection function chosen for the TPE model is EI, defined as follows:

$$EI_{y^*} = \int_{-\infty}^{y^*} (y^* - y)P(y|x)dy = \int_{-\infty}^{y^*} (y^* - y) \frac{P(y|x)P(y)}{P(x)} dy \tag{16}$$

Let  $\gamma = P(y < y^*)$  and  $\int P(y|x)P(y)dy = \gamma l(x) + (1 - \gamma)g(x)$ , construct:

$$EI_{y^*} = \frac{\gamma y^* - l(x) \int_{-\infty}^{y^*} P(y)dy}{\gamma l(x) + (1 - \gamma)g(x)} \propto \left( \gamma + \frac{g(x)}{l(x)} (1 - \gamma) \right)^{-1} \tag{17}$$

The process of determining the next sampling point is achieved by maximizing the EI function. Eq. 12 indicates that the maximum EI value is obtained when the hyperparameter  $x$  has the maximum probability of  $l(x)$  and the minimum probability of  $g(x)$ . In the TPE model, the process of maximizing EI is the process of maximizing  $\frac{g(x)}{l(x)}$ . The larger  $\frac{g(x)}{l(x)}$  is, the greater the possibility that the next sampling point  $x$  takes a value greater than  $y$  in the objective function, and the better the hyperparameter performance.

**TABLE 2 The optimal combination of super parameters of prediction models determined under different hyperparameter configuration methods.**

Algorithm	Hyperparameters	Grid search	Random search	TPE-BO	GPR-BO
XGBoost	Gamma	12	12	0.757	0
	learning_rate	0.2	0.2	0.1216	0.172
	max_depth	4	4	4	4
	n_estimators	207	208	202	211
	reg_lambda	0	0	0.002	0
	Subsample	0.9	0.9	0.935	0.947
RF	max_depth	5	9	19	16
	max_leaf_nodes	None	None	145	151
	max_samples	0.8	0.9	0.9998	0.9999
	min_samples_leaf	1	1	1	1
	min_samples_split	1	2	2	2
	min_impurity_decrease	0	0	0	0
	n_estimators	240	240	193	193
GBDT	Criterion	friedman_mse	friedman_mse	friedman_mse	mse
	learning_rate	0.15	0.15	0.2165	0.1249
	max_depth	4	4	4	4
	min_impurity_decrease	0	0	0	0
	n_estimators	231	161	239	244
	Subsample	0.9	0.9	0.9965	0.9564
KNN	Algorithm	ball_tree	ball_tree	ball_tree	ball_tree
	leaf_size	31	31	31	31
	n_neighbors	4	4	4	4
	P	1	1	1	1
	weights'	distance	distance	distance	distance
SVR	Kernel	rbf	rbf	rbf	rbf
	Gamma	0.1	0.1	0.1	0.1
	C	100	100	100	100

**TABLE 3 Performance comparison of prediction models under different hyperparameter optimization methods.**

Algorithm	Method	Grid search	Random search	TPE-BO	GPR-BO
XGBoost	Cross-validation scores	0.8486	0.8486	0.8595	0.8514
	Testing Set Score	0.7953	0.7954	0.8067	0.8182
	Search time	4,268.203s	131.0329s	137.000s	18,494.00s
RF	Cross-validation scores	0.7596	0.7595	0.7833	0.7832
	Testing Set Score	0.7580	0.7580	0.7771	0.7775
	Search time	30,566.7817s	1,180.560s	330.000s	21,767.000s
GBDT	Cross-validation scores	0.8555	0.8548	0.8669	0.8585
	Testing Set Score	0.7984	0.7897	0.7907	0.7989
	Search time	4,079.2515s	264.3815s	257.000s	22,734.000s

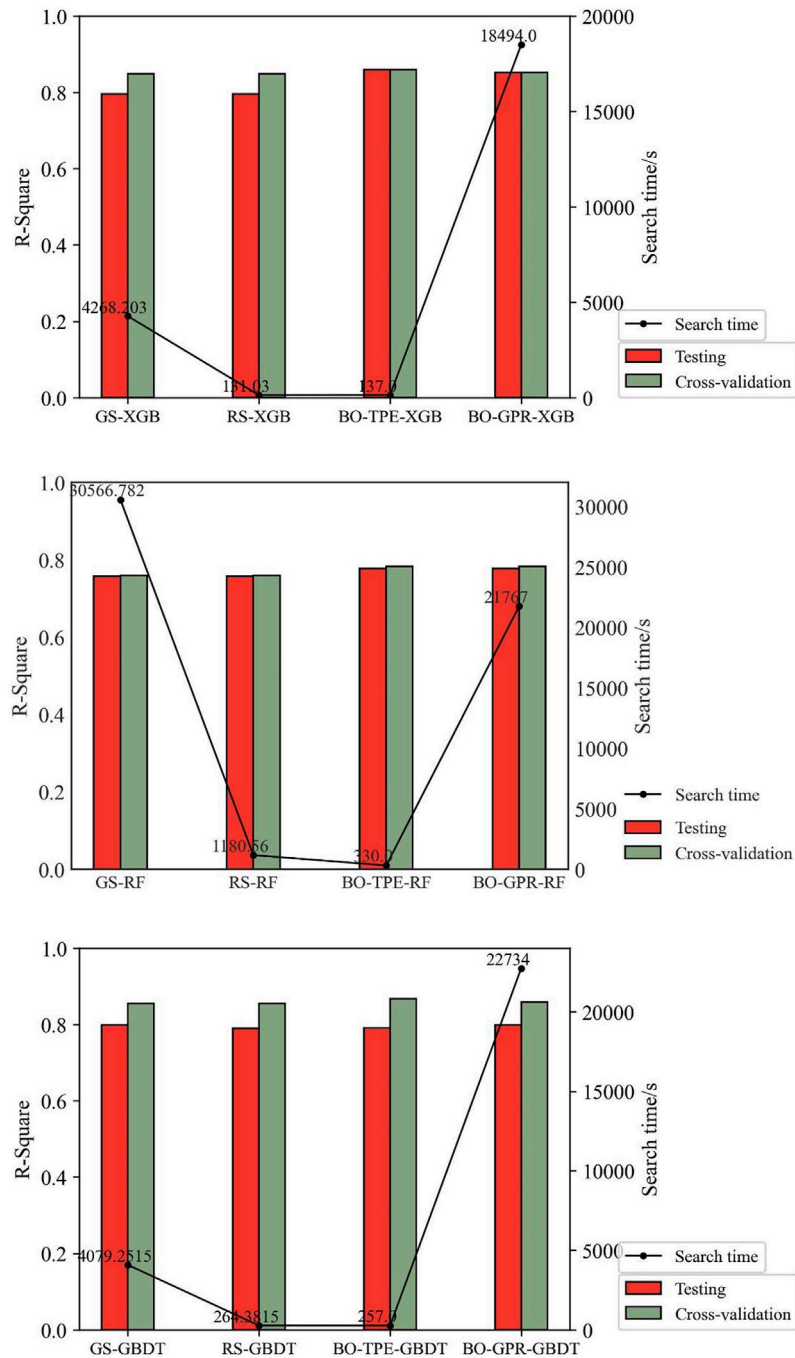


**FIGURE 9**  
Optimization Effect of Hyperparameter configuration Method in Different Models.

### 3 Experimental process

#### 3.1 Experimental framework

The RAC compressive strength prediction model's core is to use Python to access the database of RAC compressive strength, train the XGBoost, RF, KNN, SVR, and GBDT models, and then use cross-validation and the Hyperparameter configuration method (GS, RS, BO-TPE, BO-GPR) to optimize the hyperparameters in the specified hyperparameter space to produce a high-precision

RAC compressive strength prediction model. The specific process is as [Figure 6](#).

- Step 1:** The Experimental data of RAC compressive strength were collected to train the prediction model.
- Step 2:** Using Python to call the XGBoost, RF, KNN, SVR and GBDT module in the machine learning library, input the data into the model for training without adjusting the hyperparameters, and then use the model to fit the test set data to see the prediction effect.

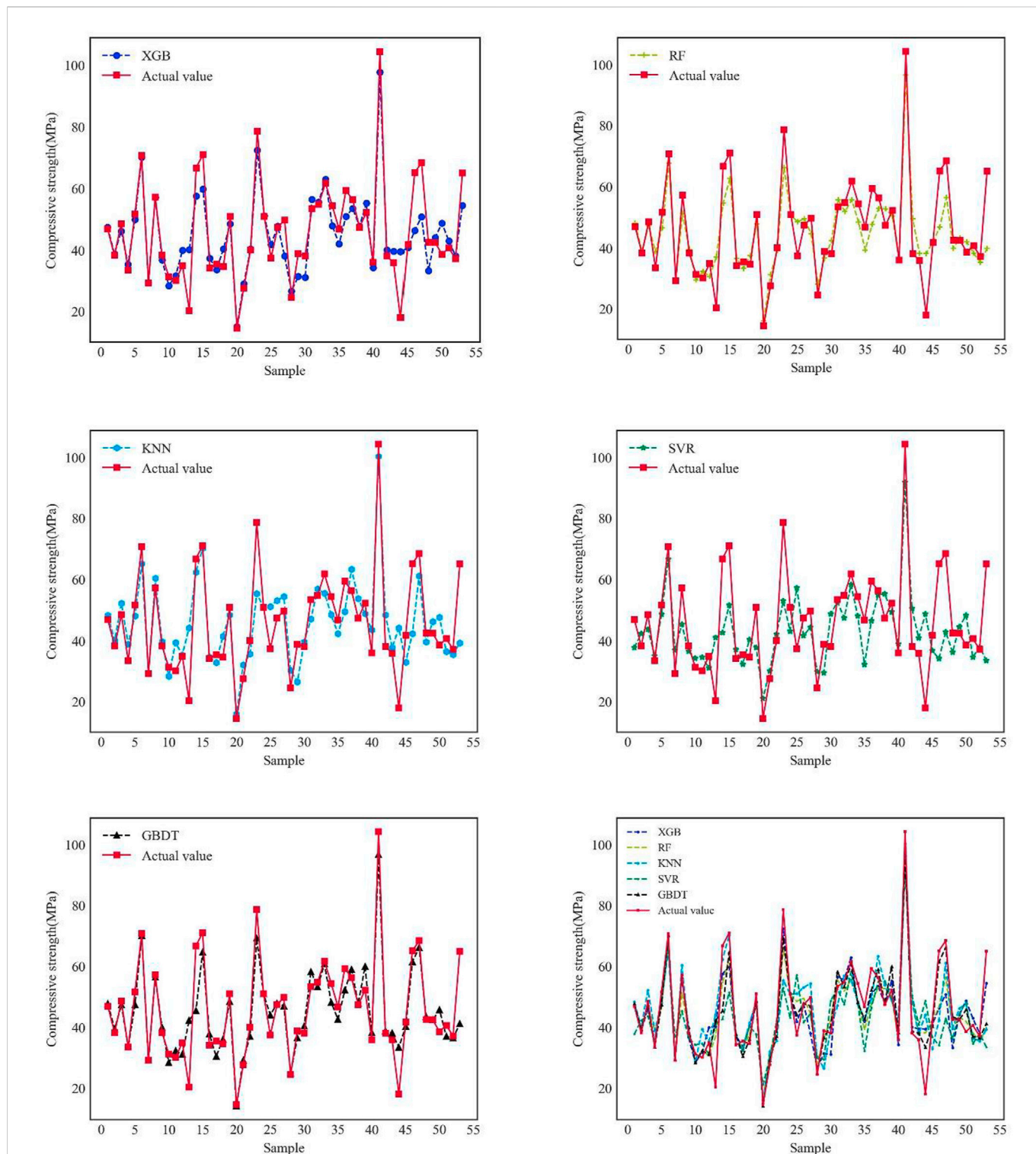


**FIGURE 10**  
Comparison of predicted values of models.

**Step 3:** Hyperparameter tuning of the models. Hyperparameter optimization is performed on the XGBoost model and RF model, KNN model, SVR model, and GBDT model using 10-fold cross-validation combined with the Hyperparameter configuration method in the training set.

**Step 4:** The optimized hyperparameters are input to each model for training. The test set data are input to the trained models, and the accuracy and generalization ability of the models are verified by calculating  $R^2$ , RMSE and MAE to compare the performance of different models.

## 3.2 Experimental procedure

### 3.2.1 Data analysis

Various studies have investigated the compressive strength (CS) of RAC. As a result, an extensive dataset with experiments on the CS of RAC was recently assembled in reference (Yuan et al., 2022). 521 of these data were selected for training and testing the machine learning model. Twelve key factors, including effective water–cement ratio ( $w_{eff}/c$ ), aggregate–cement ratio ( $a/c$ ), RCA replacement ratio ( $\rho$ ), Parent concrete strength (PCS), nominal maximum RA size ( $\delta_R$ ), nominal maximum NA size ( $\delta_N$ ), bulk density of RCA ( $m_R$ ), bulk density of NA ( $m_N$ ), water absorption of RCA ( $r_R$ ), water absorption of NA ( $r_N$ ), Los Angeles abrasion index of RCA ( $I_R$ ), Los Angeles abrasion index of NA ( $I_N$ ) were used as model inputs, and finally the model predictions of the compressive strength of RAC were output. Table 1 shows the mean, median, maximum, and minimum values of the data used in this study. The distribution of the data used in this paper is shown in Figure 7. The effective water–cement ratio is mainly distributed in 0.3–0.6; the aggregate–cement ratio is mainly distributed in 2–4; the replacement rate of RAC mainly takes values around 0%, 20%, 50% and 30%; The Parent concrete strength ranged from 0 MPa to 75 MPa; The nominal maximum NA size and the nominal maximum NA size is mainly distributed in 15 mm–30 mm; The bulk density of RCA and the bulk density of NA ranged from 2,500/kg m<sup>3</sup> to 3,000/kg m<sup>3</sup>; the water absorption of RCA is mainly distributed in 4%–8%; the water absorption of NA is mainly distributed in 0.3%–1.5%; Los Angeles abrasion index of RCA ranges from 30 to 45 MPa; Los Angeles abrasion index of NA ranged from 20 to 35.

Figure 8 illustrates the multiple correlation matrix of the input parameters and outputs used in this study. The shades of color indicate the magnitude of the correlations. Among the input variables, the highest correlation was found between bulk density of RCA ( $m_R$ ) and water absorption of RCA ( $r_R$ ),  $R=0.74$ ; followed by the correlation between bulk density of NA ( $m_N$ ) and water absorption of NA ( $r_N$ ) of 0.7; The correlation coefficient between RCA replacement ratio ( $\rho$ ) and bulk density of RCA ( $m_R$ ) is 0.59; The correlation coefficient between RCA replacement ratio ( $\rho$ ) and water absorption of RCA ( $r_R$ ) is 0.46. The larger the RAC replacement rate, the more mortar adhered to the surface of RAC with higher water absorption (Chakradhara Rao et al., 2011; McNeil and Kang, 2013; Duan and Poon, 2014). Between the input and output variables, the correlation between the Parent concrete strength (PCS) and the compressive strength (CS) of RAC was the largest. Furthermore, the correlation between the input and output variables was relatively low overall. As a result, all input variables were chosen in this study to improve the predictive model's accuracy.

### 3.2.2 Hyperparameter configuration

The grid search algorithm brings all the parameter combinations in the parameter space into the model for training. The grid search algorithm traverses each parameter combination, which consumes a lot of computational resources; the random grid search selects some parameter combinations as “subspace” by non-relaxed sampling and searches only these parameter combinations. The hyperparameter combinations are shown in Table 2. Bayesian optimization is a state-of-the-art automated method for tuning parameters, which proceeds as follows:

- Step 1:** According to the determined parameter space, randomly generate hyperparameter combinations  $X = [x_1, x_2, x_3, x_4 \dots x_n]$  within the hyperparameter taking values, substitute them into the data set, and train the prediction model to obtain the corresponding objective function of the parameter combinations, i.e., the cross-validation assessment index ( $R^2$ );  $Y = [f(x_1), f(x_2), f(x_3), f(x_4) \dots f(x_n)]$  form the initial hyperparameter and prediction accuracy data set.
- Step 2:** The sample points are classified as good or poor based on the prediction accuracy dataset, and an agent model is built.
- Step 3:** The next set of hyperparameter sampling points  $x_{n+1}$  is sought from the proxy model based on the EI acquisition function. The hyperparameter combination is substituted into the data set for training to obtain the predicted values of the compressive strength of recycled concrete with the cross-validation evaluation index  $f(x_{n+1})$ .
- Step 4:** If the cross-validation assessment index meets the requirements,  $f(x_{n+1})$  is used as the best hyperparameter most and the procedure is terminated.

### 3.2.3 Model evaluation

After the prediction model is built, its performance needs to be evaluated. The model evaluation indexes used in this paper are: correlation coefficient ( $R^2$ ), Root Mean Square Error (RMSE), and mean absolute error (MAE). Of these,  $R^2$  judges the feasibility and linearity of the model; MAE reflects the mean of the absolute errors between the predicted and actual values; RMSE represents the square root of the second order sample moments of the difference between the predicted and observed values, the equation is as follows:

$$R^2 = 1 - \frac{\sum_i (y_i - f_i)^2}{\sum_i (y_i - \bar{y})^2} \quad (18)$$

$$\bar{y} = \frac{1}{n} \sum_{i=1}^n y_i \quad (19)$$

$$RMSE = \sqrt{\frac{1}{n} \sum_{i=1}^n (y_i - f_i)^2} \quad (20)$$

$$MAE = \frac{1}{n} \sum_{i=1}^n |y_i - f_i| \quad (21)$$

Where:  $n$  is the total number of samples involved in the training;  $y_i$  is the measured value of the strength of RAC in group  $i$ ;  $f_i$  is the predicted value of RAC in group  $i$ .

## 4 Results and analysis

### 4.1 Analysis of the impact of hyperparametric configuration methods on model performance

The grid search hyperparameters consume more computational resources for the same parameter space. Therefore, the grid search hyperparameter space is smaller than the Bayesian optimization hyperparameter space. The grid search hyperparameter space is the same as the random search hyperparameter space. This makes it easier to compare how different hyperparameter optimization methods affect how well a model works. Moreover, the number of iterations is the same for Gaussian Process (GP)-based Bayesian optimization

TABLE 4 Performance comparison of prediction models of different RA concrete.

		XGBoost	RF	KNN	SVR	GBDT
$R^2$	Training	0.9980	0.9707	0.9980	0.5982	0.9995
	Testing	0.8067	0.7770	0.6744	0.4114	0.7907
	Cross-validation	0.8595	0.7833	0.6664	0.5499	0.8669
RMSE	Training	0.6774	2.6264	0.3455	9.7215	0.3474
	Testing	7.1011	7.6264	9.2161	12.3920	7.3897
	Cross-validation	13.6706	13.3683	14.5179	14.1952	15.4523
MAE	Training	0.4840	1.9523	0.0560	7.3493	0.0563
	Testing	4.7576	5.3456	6.5160	9.2291	4.4714
	Cross-validation	10.7253	10.8279	11.5830	11.4475	11.8661

and TPE-based Bayesian optimization, which is 1,000 iterations. The optimization effect of the hyperparameter configuration method in different models is shown in Figure 9 and Table 3.

The grid and the random search methods are essentially enumerative, with a similar combination of hyperparameters searched and not much difference in cross-validation scores. However, because the search space of random search is only a subspace of the full domain space, the hyperparameter search time is substantially reduced compared with grid search, and the speed of random search is 15–32 times faster than grid search in this experiment. The larger the hyperparameter search space and the more complex the model, the more significant the difference in search time between the two. The performance of the prediction models under TPE-based Bayesian optimization was better than that of the grid search method and the random grid search method, and the fit of the XGBoost, RF, and GBDT models increased by 0.00109, 0.0238, and 0.004, respectively. The performance of the prediction models under TPE-based Bayesian hyperparameter optimization was better than that of GPR-based Bayesian hyperparameter optimization. In the prediction models under Bayesian hyperparameter optimization, the degree of fit of XGBoost, RF, and GBDT models increased by 0.0081, 0.0001, and 0.0084 in turn, and was faster, with the average search time of the TPE method being about 241 s and the average search time of the GPR method being 20,998 s. In this experiment, the TPE-BO hyperparameter optimization method reduced the search time by a factor of 65–134 compared to the GPR-BO method.

## 4.2 Comparative analysis of the performance of different models

The comparison graphs of the predicted values of different models are shown in Figure 10. All the following prediction models adopt BO-TPE super-parameter configuration method. As seen from the figure, the predicted values of the SVR prediction model deviate significantly from the actual values. In each prediction model, the predicted values of sample 12 and sample 44 deviated substantially from the true values, with a relative error of up to 140%, possibly because the sample was an outlier. Excluding the above abnormal samples, the KNN prediction model

is unstable, with a minimum relative error of 3.18% and a maximum relative error of 39.62% between the predicted and true values; the deviations between the predicted and true values of the XGBoost, RF and GBDT models were relatively small, with an average relative error of 12.2%, 13.02%, and 10.94% for each model respectively; the minimum relative error between the predicted and actual values was 0.24% for the XGBoost model, 0.16% for the RF model and 0% for the GBDT model. Ensemble learning models outperform individual learning models, and the GBDT model has the smallest deviation from the true value and the highest prediction accuracy of any Ensemble learning model.

As seen in Table 4, Figure 11, the cross-validation  $R^2$  score for the GBDT model was the highest, being 0.0074, 0.0836, 0.1925, and 0.317 more heightened than the XGB, RF, KNN, and SVR models, respectively. Therefore, the GBDT model has better fitting and generalization capabilities, followed by the XGBoost model, RF model, KNN model, and SVM model. The cross-validation  $R^2$  scores and training set  $R^2$  scores of the XGBoost, SVR, and GBDT models were all higher than the test set scores, which shows that the overall prediction effect of the models was higher than the prediction effect in the test set, and the models did not predict well in this randomly selected test set. The cross-validation  $R^2$  scores and training set  $R^2$  scores of the RF and KNN models were not significantly different from the test set scores. The model normally performed in prediction on this randomly selected test set. The XGBoost, RF, and GBDT models have smaller differences between training set  $R^2$  and test set  $R^2$  than the other models. Their generalization error and empirical error balance are higher than the other models. The single model learning has higher empirical risk and easy overfitting compared to integrated learning (XGBoost, RF, GBDT); The training set  $R^2$  of the KNN model is larger than the test set, and the training set  $R^2$  of the SVR model is smaller than the test set  $R^2$ . The SVR model may have structural risk.

The RMSE evaluates the degree of variability in the data, with smaller values of RMSE indicating that the predictive model describes the experimental data with better accuracy. The prediction models in descending order of RMSE are the RF model, XGBoost model, SVR model, KNN model, and GBDT model with RMSE of 13.37, 13.47, 14.2, 14.52, and 15.45, respectively. The RF, SVR, and XGBoost models have better data description capability. The KNN and GBDT models have a large RMSE and may be affected by outliers.

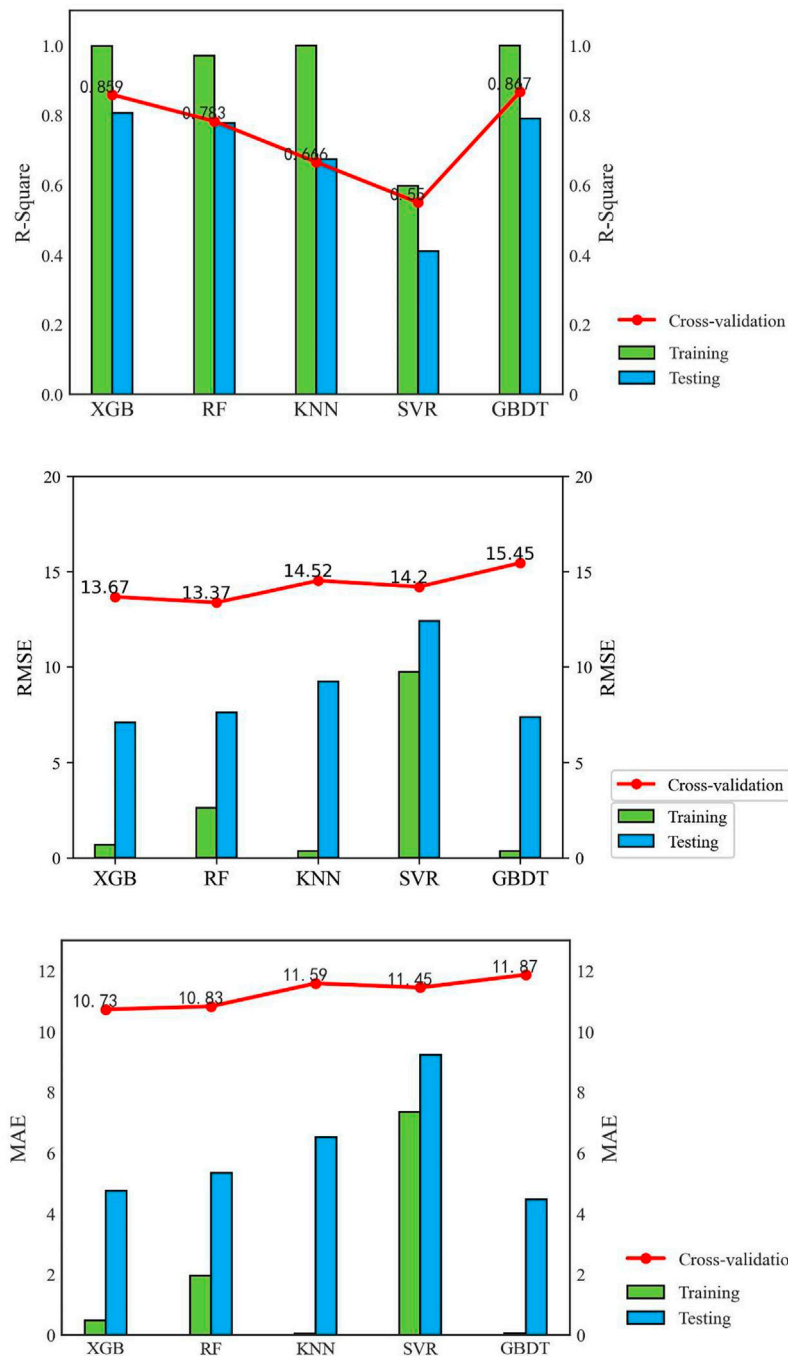


**FIGURE 11**  
Comparison of model prediction performance.

The MAE indicator avoids the problem of forecast deviations and true values canceling each other out. The MAE of each model was not very different, and the smallest XGBoost model. The MAE of the XGBoost model was smaller than the RF model, KNN model, SVR model, and GBDT model by 0.1, 0.86, 0.72, and 1.14 respectively.

The average  $R^2$  of the cross-validation set for each prediction model is smaller than the training and validation sets, and the average RMSE and MAE are larger than the training and validation sets. The possible reasons for this are 1. The small size of the recycled coarse aggregate concrete sample data; 2. Insufficient relevant features given

about recycled coarse aggregate concrete; and 3. The presence of outliers in the collected data. Collecting additional data and features for model training and improving the model's generalization capability is necessary.

### 4.3 Feature sensitivity analysis

The objectives of the work are to 1) Determine the importance of each input parameter to the compressive strength of the RAC (Medina

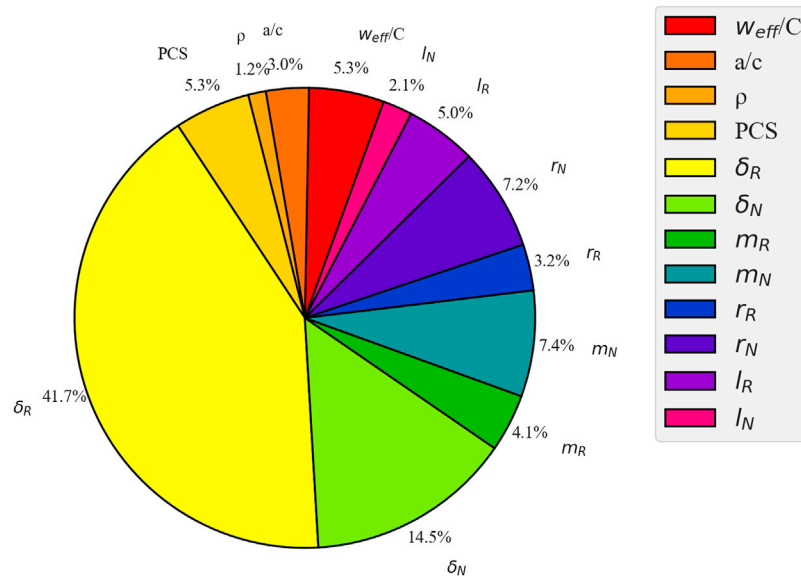


**FIGURE 12**  
Ranking of feature importance of XGBoost Model.

et al., 2021). 2) Quantitatively calculating the importance of different features affecting the compressive strength of RAC helps to understand the intrinsic mechanism of the compressive strength of RAC. XGBoost prediction model ranks the importance of different features affecting the strength of concrete, and their results are shown in Figure 12.

The feature importance ranking in the XGBoost prediction model is nominal maximum RA size ( $\delta_R$ ), nominal maximum NA size ( $\delta_N$ ), bulk density of NA ( $m_N$ ), water absorption of NA ( $r_N$ ), effective water–cement ratio ( $w_{eff}/c$ ), Parent concrete strength (PCS), Los Angeles abrasion index of RCA ( $l_R$ ), bulk density of RCA ( $m_R$ ), water absorption of RCA ( $r_R$ ), aggregate–cement ratio ( $a/c$ ), Los Angeles abrasion index of NA ( $l_N$ ), RCA replacement ratio ( $\rho$ ). The importance of nominal maximum RA size ( $\delta_R$ ) and nominal maximum NA size ( $\delta_N$ ) is 41.7% and 14.5%, respectively, two characteristics strongly related to the crushing index of the aggregates. The physicochemical mechanism of compressive strength of concrete, fracture, and energy dissipation of recycled aggregate concrete material is a central physical mechanism (Bai et al., 2021; Bai et al., 2023). The crushing index is an essential parameter of aggregate strength. Because of the RAC the surface roughness, internal cracks, and other characteristics make its crushing index higher than that of NA, and its contribution to the compressive strength of RAC is lower than that of NA. The importance of water absorption of NA ( $r_N$ ) and water absorption of RCA ( $r_R$ ) is 7.2% and 3.2% respectively. Studies have shown that the water absorption of RAC is greater than that of NA and that less absorbent aggregates have higher strength RAC (Koper et al., 2017). The importance of the bulk density of RAC ( $m_R$ ) and the bulk density of NA ( $m_N$ ) is 4.1% and 7.4% respectively. The bulk density of RAC is lower than NA. RAC has a looser internal structure, greater porosity than NA, and therefore, greater water absorption and lower compressive strength (Wagih et al., 2013). The importance of the Los Angeles abrasion index of RCA ( $l_R$ ) and Los Angeles abrasion index of NA ( $l_N$ ) is 5.0% and 2.1%, respectively. The Los Angeles abrasion index measures the quality of the aggregate, with a higher A meaning a less abrasive aggregate. The RAC aggregate has lower

compressive and abrasion resistance than the NA due to the loss of virgin aggregate in the RAC separation and fragmentation of the mortar attached to the exterior of the RAC (González-Taboada et al., 2016; Park et al., 2018). The importance of the effective water–cement ratio ( $w_{eff}/c$ ) on the compressive strength of RAC is 5.3%. The larger the  $w_{eff}/c$ , the more free water inside RAC, and the evaporation of free water will form small pores inside RAC, making the compressive strength of RAC become smaller. The importance of PCS is 5.3%, and many experimental results show that RAC made from recycled aggregates derived from high-strength parent concrete has a higher compressive strength than RAC made from recycled aggregates derived from normal parent concrete (Kou and Poon, 2015; Chakradhara Rao, 2018; Ahmad Bhat, 2021).

## 5 Conclusion

In this study, Bayesian optimization methods were used to tune the hyperparameters of the machine learning model to predict the non-linear relationship between the compressive strength of the RAC and the relevant influencing factors. The following conclusions were drawn:

- (1) Based on the TPE-BO hyperparameter optimization method, the performance of the RAC compressive strength prediction model is effectively improved, and the efficiency is higher than other hyperparameter optimization methods.
- (2) The TPE-BO optimized model was put to predict the compressive strength of RAC, and the TPE-BO-GBDT model obtained a higher prediction accuracy with a 10-fold cross-validation  $R^2 = 0.8669$  when comparing the  $R^2$ , RMSE, and MAE of different models.
- (3) The ranking of the importance of the features affecting the compressive strength of RAC are:  $\delta_R$ ,  $\delta_N$ ,  $m_N$ ,  $r_N$ ,  $w_{eff}/c$ , PCS,  $l_R$ ,  $m_R$ ,  $r_R$ ,  $a/c$ ,  $l_N$ ,  $\rho$ , and this conclusion can provide a reference for the subsequent selection of features.

Although this paper only discusses the use of machine learning combined with Bayesian optimization in predicting the compressive strength of RAC, the TPE-BO optimization machine learning approach proposed in this paper can be extended to predict the mechanical properties of other types of concrete. In future work, we will collect more RAC experimental data and related influencing factors and try more hyperparameters optimization methods, such as PSO, GWO algorithm, and Differential Evolution (DE), to improve the accuracy and efficiency of the model prediction.

## Data availability statement

Publicly available datasets were analyzed in this study. This data can be found here: <https://www.mdpi.com/article/10.3390/ma15082823/s1>.

## Author contributions

ZX carried out the main writing of the article and the content of numerical test. DC revised the structure of the article and provided financial support. LW and CY has sorted out the references and layout of the article.

## References

- Ahmad Bhat, J. (2021). Effect of strength of parent concrete on the mechanical properties of recycled aggregate concrete. *Mater. Today Proc.* 42, 1462–1469. doi:10.1016/j.matpr.2021.01.310
- Alam, M. S., Sultana, N., and Hossain, S. Z. (2021). Bayesian optimization algorithm based support vector regression analysis for estimation of shear capacity of FRP reinforced concrete members. *Appl. Soft Comput.* 105, 107281. doi:10.1016/j.asoc.2021.107281
- Alhakeem, Z. M., Jebur, Y. M., Henedy, S. N., Imran, H., Bernardo, L. F., and Hussein, H. M. (2022). Prediction of ecofriendly concrete compressive strength using gradient boosting regression tree combined with GridSearchCV hyperparameter-optimization techniques. *Materials* 15 (21), 7432. doi:10.3390/ma15217432
- Awad, M., and Khanna, R. (2015). "Support vector regression," in *Efficient learning machines* (Berlin, Germany: Springer), 67–80.
- Bai, B., Zhou, R., Cai, G., Hu, W., and Yang, G. (2021). Coupled thermo-hydro-mechanical mechanism in view of the soil particle rearrangement of granular thermodynamics. *Comput. Geotechnics* 137, 104272. doi:10.1016/j.compgeo.2021.104272
- Bai, B., Zhou, R., Yang, G., Zou, W., and Yuan, W. (2023). The constitutive behavior and dissociation effect of hydrate-bearing sediment within a granular thermodynamic framework. *Ocean. Eng.* 268, 113408. doi:10.1016/j.oceaneng.2022.113408
- Bai, G., Zhu, C., Liu, C., and Liu, B. (2020). An evaluation of the recycled aggregate characteristics and the recycled aggregate concrete mechanical properties. *Constr. Build. Mater.* 240, 117978. doi:10.1016/j.conbuildmat.2019.117978
- Basak, D., Pal, S., and Patranabis, D. C. (2007). Support vector regression. *Statistics Comput.* 11 (10).
- Bergstra, J., Bardenet, R., Bengio, Y., and Kégl, B. (2011). Algorithms for hyperparameter optimization. *Adv. neural Inf. Process. Syst.* 24.
- Bergstra, J., and Bengio, Y. (2012). Random search for hyper-parameter optimization. *J. Mach. Learn. Res.* 13 (2).
- Bergstra, J., Yamins, D., and Cox, D. (2013). "Making a science of model search: Hyperparameter optimization in hundreds of dimensions for vision architectures," in Proceedings of the International conference on machine learning: PMLR, Atlanta, Georgia, USA, June 2013, 115–123.
- Breiman, L. (2001). Random forests. *Mach. Learn.* 45 (1), 5–32. doi:10.1023/a:1010933404324
- Catherina, V. P., and Chella, K. N. (2021). Prediction of compressive strength of recycled aggregate concrete using artificial neural network and cuckoo search method. *Mater. Today Proc.* 46, 8480–8488. doi:10.1016/j.matpr.2021.03.500
- Chakradhara Rao, M., Bhattacharyya, S., and Barai, S. (2011). Influence of field recycled coarse aggregate on properties of concrete. *Mater. Struct.* 44 (1), 205–220. doi:10.1617/s11527-010-9620-x
- Chakradhara Rao, M. (2018). Properties of recycled aggregate and recycled aggregate concrete: Effect of parent concrete. *Asian J. Civ. Eng.* 19 (1), 103–110. doi:10.1007/s42107-018-0011-x
- Chen, T., and Guestrin, C. (2016). "Xgboost: A scalable tree boosting system," in Proceedings of the 22nd acm sigkdd international conference on knowledge discovery and data mining, San Francisco, CA, USA, August 2016, 785–794.
- Duan, Z.-H., Kou, S.-C., and Poon, C.-S. (2013). Prediction of compressive strength of recycled aggregate concrete using artificial neural networks. *Constr. Build. Mater.* 40, 1200–1206. doi:10.1016/j.conbuildmat.2012.04.063
- Duan, Z., and Poon, C. (2014). Properties of recycled aggregate concrete made with recycled aggregates with different amounts of old adhered mortars. *Mater. Des.* 58, 19–29. doi:10.1016/j.matdes.2014.01.044
- Eggensperger, K., Hutter, F., Hoos, H., and Leyton-Brown, K. (2015). "Efficient benchmarking of hyperparameter optimizers via surrogates," in Proceedings of the AAAI Conference on Artificial Intelligence, Austin, TX, USA, January 2015.(.)
- Feurer, M., and Hutter, F. (2019). "Hyperparameter optimization," in *Automated machine learning* (Berlin, Germany: Springer), 3–33.
- Freund, Y., Schapire, R., and Abe, N. (1999). A short introduction to boosting. *Journal-Japanese Soc. Artif. Intell.* 14 (771-780), 1612. .
- Friedman, J. H. (2001). Greedy function approximation: A gradient boosting machine. *Ann. statistics* 29, 1189–1232. doi:10.1214/aos/1013203451
- Giesekam, J., Barrett, J. R., and Taylor, P. (2016). Construction sector views on low carbon building materials. *Build. Res. Inf.* 44 (4), 423–444. doi:10.1080/09613218.2016.1086872
- González-Taboada, I., González-Fontoeba, B., Martínez-Abella, F., and Carro-López, D. (2016). Study of recycled concrete aggregate quality and its relationship with recycled concrete compressive strength using database analysis. *Materiales de Construcción* 66 (323), e099. doi:10.3989/mc.2016.06415
- Gull, I. (2011). Testing of strength of recycled waste concrete and its applicability. *J. Constr. Eng. Manag.* 137 (1), 1–5. doi:10.1061/(asce)co.1943-7862.0000255
- Guo, Z., Chen, L., Gui, L., Du, J., Yin, K., and Do, H. M. (2020a). Landslide displacement prediction based on variational mode decomposition and WA-GWO-BP model. *Landslides* 17 (3), 567–583. doi:10.1007/s10346-019-01314-4
- Guo, Z., Chen, L., Yin, K., Shrestha, D. P., and Zhang, L. (2020b). Quantitative risk assessment of slow-moving landslides from the viewpoint of decision-making: A case study of the three gorges reservoir in China. *Eng. Geol.* 273, 105667. doi:10.1016/j.enggeo.2020.105667
- Khademi, F., Jamal, S. M., Deshpande, N., and Londhe, S. (2016). Predicting strength of recycled aggregate concrete using artificial neural network, adaptive neuro-fuzzy inference system and multiple linear regression. *Int. J. Sustain. Built Environ.* 5 (2), 355–369. doi:10.1016/j.ijsbe.2016.09.003
- Koper, A., Koper, W., and Koper, M. (2017). Influence of raw concrete material quality on selected properties of recycled concrete aggregates. *Procedia Eng.* 172, 536–543. doi:10.1016/j.proeng.2017.02.063

## Funding

This research was completed under the support of the GuangXi Key Laboratory of New Energy and Building Energy Saving.

## Conflict of interest

The authors declare that the research was conducted in the absence of any commercial or financial relationships that could be construed as a potential conflict of interest.

## Publisher's note

All claims expressed in this article are solely those of the authors and do not necessarily represent those of their affiliated organizations, or those of the publisher, the editors and the reviewers. Any product that may be evaluated in this article, or claim that may be made by its manufacturer, is not guaranteed or endorsed by the publisher.

- Kou, S.-c., and Poon, C.-s. (2015). Effect of the quality of parent concrete on the properties of high performance recycled aggregate concrete. *Constr. Build. Mater.* 77, 501–508. doi:10.1016/j.conbuildmat.2014.12.035
- Li, Y., and Chen, W. (2020). A comparative performance assessment of ensemble learning for credit scoring. *Mathematics* 8 (10), 1756. doi:10.3390/math8101756
- Liang, W., Luo, S., Zhao, G., and Wu, H. (2020). Predicting hard rock pillar stability using GBDT, XGBoost, and LightGBM algorithms. *Mathematics* 8 (5), 765. doi:10.3390/math8050765
- Liu, Y., Wang, Y., and Zhang, J. (2012). “New machine learning algorithm: Random forest,” in Proceedings of the International Conference on Information Computing and Applications, Wuhan, China, October 2012, 246–252.
- McNeil, K., and Kang, T. H.-K. (2013). Recycled concrete aggregates: A review. *Int. J. Concr. Struct. Mater.* 7 (1), 61–69. doi:10.1007/s40069-013-0032-5
- Medina, V., Hürlimann, M., Guo, Z., Lloret, A., and Vaunat, J. (2021). Fast physically-based model for rainfall-induced landslide susceptibility assessment at regional scale. *Catena* 201, 105213. doi:10.1016/j.catena.2021.105213
- Meng, T., Wei, H., Yang, X., Zhang, B., Zhang, Y., and Zhang, C. (2021). Effect of mixed recycled aggregate on the mechanical strength and microstructure of concrete under different water cement ratios. *Materials* 14 (10), 2631. doi:10.3390/ma14102631
- Nunez, I., Marani, A., and Nehdi, M. L. (2020). Mixture optimization of recycled aggregate concrete using hybrid machine learning model. *Materials* 13 (19), 4331. doi:10.3390/ma13194331
- Ozaki, Y., Tanigaki, Y., Watanabe, S., and Onishi, M. (2020). “Multiobjective tree-structured parzen estimator for computationally expensive optimization problems,” in Proceedings of the 2020 genetic and evolutionary computation conference, Cancun Mexico, July 2020, 533–541.
- Park, S. S., Kim, S. J., Chen, K. Q., Lee, Y. J., and Lee, S. B. (2018). Crushing characteristics of a recycled aggregate from waste concrete. *Constr. Build. Mater.* 160, 100–105. doi:10.1016/j.conbuildmat.2017.11.036
- Peterson, L. E. (2009). K-nearest neighbor. *Scholarpedia* 4 (2), 1883. doi:10.4249/scholarpedia.1883
- Quinlan, J. R. (1986). Induction of decision trees. *Mach. Learn.* 1 (1), 81–106. doi:10.1007/bf00116251
- Rakshvir, M., and Barai, S. V. (2006). Studies on recycled aggregates-based concrete. *Waste Manag. Res.* 24 (3), 225–233. doi:10.1177/0734242x06064820
- Rasmussen, C. E. (2003). “Gaussian processes in machine learning,” in *Summer school on machine learning* (Berlin, Germany: Springer), 63–71.
- Rasmussen, C. E., and Nickisch, H. (2010). Gaussian processes for machine learning (GPML) toolbox. *J. Mach. Learn. Res.* 11, 3011–3015.
- Ray, S. (2019). “A quick review of machine learning algorithms,” in Proceedings of the 2019 International conference on machine learning, big data, cloud and parallel computing (COMITCon): IEEE, Faridabad, India, February 2019, 35–39.
- Schölkopf, B., Smola, A. J., Williamson, R. C., and Bartlett, P. L. (2000). New support vector algorithms. *Neural Comput.* 12 (5), 1207–1245. doi:10.1162/089976600300015565
- Sen, P. C., Hajra, M., and Ghosh, M. (2020). “Supervised classification algorithms in machine learning: A survey and review,” in *Emerging technology in modelling and graphics* (Berlin, Germany: Springer), 99–111.
- Sev, A. (2009). How can the construction industry contribute to sustainable development? A conceptual framework. *Sustain. Dev.* 17 (3), 161–173. doi:10.1002/sd.373
- Shi, F., Huang, T., Tanikawa, H., Han, J., Hashimoto, S., and Moriguchi, Y. (2012). Toward a low carbon–dematerialization society: Measuring the materials demand and CO<sub>2</sub> emissions of building and transport infrastructure construction in China. *J. Industrial Ecol.* 16 (4), 493–505. doi:10.1111/j.1530-9290.2012.00523.x
- Silva, R., de Brito, J., and Dhir, R. (2015). The influence of the use of recycled aggregates on the compressive strength of concrete: A review. *Eur. J. Environ. Civ. Eng.* 19 (7), 825–849. doi:10.1080/19648189.2014.974831
- Smola, A. J., and Schölkopf, B. (2004). A tutorial on support vector regression. *Statistics Comput.* 14 (3), 199–222. doi:10.1023/b:stco.0000035301.49549.88
- Spence, R., and Mulligan, H. (1995). Sustainable development and the construction industry. *Habitat Int.* 19 (3), 279–292. doi:10.1016/0197-3975(94)00071-9
- Vapnik, V., Golowich, S., and Smola, A. (1996). Support vector method for function approximation, regression estimation and signal processing. *Adv. neural Inf. Process. Syst.* 9.
- Wagih, A. M., El-Karmoty, H. Z., Ebid, M., and Okba, S. H. (2013). Recycled construction and demolition concrete waste as aggregate for structural concrete. *HBRC J.* 9 (3), 193–200. doi:10.1016/j.hbrj.2013.08.007
- Wang, Y., Li, X., Wang, Z., and Liu, J. (2022a). Deep learning for magnitude prediction in earthquake early warning. *Gondwana Res.* doi:10.1016/j.gr.2022.06.009
- Wang, Y., Zhao, Q., Li, Y., Zhang, M., and Zhu, W. (2022b). Detecting cable force anomalies on cable-stayed bridges using the STA/LTA method. *Sustainability* 14 (18), 11373. doi:10.3390/su141811373
- Xia, B., Olanipekun, A., Chen, Q., Xie, L., and Liu, Y. (2018). Conceptualising the state of the art of corporate social responsibility (CSR) in the construction industry and its nexus to sustainable development. *J. Clean. Prod.* 195, 340–353. doi:10.1016/j.jclepro.2018.05.157
- Ying, J., Su, F., and Chen, S. (2022). Long term performance of recycled concrete beams with different water–Cement ratio and recycled aggregate replacement rate. *Front. Struct. Civ. Eng.* 16, 302–315. doi:10.1007/s11709-022-0803-7
- Yuan, X., Tian, Y., Ahmad, W., Ahmad, A., Usanova, K. I., Mohamed, A. M., et al. (2022). Machine learning prediction models to evaluate the strength of recycled aggregate concrete. *Materials* 15 (8), 2823. doi:10.3390/ma15082823
- Zhang, L., Li, Q., and Zhou, J. (2017). Critical factors of low-carbon building development in China’s urban area. *J. Clean. Prod.* 142, 3075–3082. doi:10.1016/j.jclepro.2016.10.160
- Zhang, Y., Kang, J., and Jin, H. (2018). A review of green building development in China from the perspective of energy saving. *Energies* 11 (2), 334. doi:10.3390/en11020334